Load Frequency Control Strategy of Interconnected Power System Based on Tube DMPC

Wang Xinshan

School of control and computer engineering, North China Electric Power University, Beijing 102206, China
E-mail: 18810240204@163.com

Received 25 March 2024; Accepted 15 April 2024

Abstract

Solar thermal power generation shares technical characteristics with traditional thermal power generation. This enables rapid adjustment of turbine generator output to meet the demands of the power grid load for frequency modulation. However, fluctuations in light intensity lead to variations in interconnected power system parameters, posing challenges for load frequency control (LFC). In this study, we propose a Robust Distributed Model Predictive Control (RDMPC) method. This method achieves system trajectory tracking by solving the nominal system optimization problem. It also flexibly adjusts the weights of different Tube models to determine the optimal control law using the standard Tube online combination with various gain values. Additionally, we incorporate the states of adjacent areas into the feedback control law to achieve effective coordination between these areas. Using

Distributed Generation & Alternative Energy Journal, Vol. 39_3, 635–658.
doi: 10.13052/dgaej2156-3306.39311

MATLAB/Simulink, we simulated the power system in two areas. Compared to standard Tube DMPC, our proposed algorithm effectively mitigates the impact of light intensity, enhances adjustment speed, reduces frequency fluctuation, and demonstrates superior control effectiveness.

Keywords: Robust model predictive control, load frequency control, uncertain parameters.

1 Introduction

Load frequency control is crucial for maintaining the stability of power systems. Its primary function is to regulate frequency deviation within specified limits by adjusting the power output of generator sets in response to load changes, thus ensuring system frequency stability [1]. With the promotion of the "double carbon" goal, the proportion of high-proportion, intermittent and volatile new energy generation in the power system is increasing, and the shortcomings and problems such as insufficient flexibility of frequency control and insufficient adjustment capacity of the power system are becoming increasingly prominent. Solar thermal power plant (STPP) offers real-time control over power output by adjusting the working state of reflectors or turbine generator sets. This capability enables it to effectively manage frequency fluctuations in the power system, offering high adjustability and flexibility. STPPs play a pivotal role in the transition towards a new energy-centric power system, ensuring its safe and stable operation [2].

Distributed Model Predictive Control (DMPC) has emerged as a powerful technique for enhancing the stability, robustness, and response speed of systems, finding extensive application in Load Frequency Control within modern multi-area interconnected power systems [3]. DMPC divides the entire system into multiple subsystems, each equipped with an independent controller capable of adjusting its state autonomously. This approach enables rapid and efficient to the distributed control needs of the power system. NONG Huiyun [4] established a multi-regional interconnected power system model composed of wind power, photovoltaic power and thermal power. Using DMPC they regulated the frequency and power of interconnection lines to remain within specified limits. However, this control strategy overlooked the influence of changes in wind speed and light intensity on the system, thereby exhibiting certain limitations. In another study, Liao Xiaobing

et al. [5] proposed a collaborative distributed model predictive control algorithm for LFC of power system under the access of photothermal system. This algorithm coordinated the output power of each area to accommodate load changes. Nevertheless, it adopted the known sequence of light intensity changes, which had limitations in practical application. The fluctuation of light intensity alters the LFC model parameters, reducing system frequency stability and heightening the need for coordinated control among diverse power generation systems. This underscores the imperative for ensuring the safe and stable operation of the power grid.

The robust distributed model predictive control (RDMPC) has been widely used in many engineering fields due to its robustness, effectiveness, high flexibility, good control effect, easy implementation and expansion. Zhang Yi et al. [6] proposes a robust distributed LFC strategy for interconnected power systems with parameter uncertainty and structure uncertainty. This strategy reformulates the optimization problem into the solution of linear matrix inequalities, enabling global optimal control while satisfying constraints. Liu Xiangjie et al. [7] proposes Tube DMPC control strategy to address the uncertainty of wind speed. It uses the combination of DMPC and feedback control law to limit the state change of the system within a certain range, thereby minimizing the impact of wind speed disturbance on the system and fostering effective coordination between areas. Nonetheless, this strategy's utilization of fixed feedback gains implies limited flexibility, potentially leading to scenarios where viable solutions may be elusive.

In this paper, a Robust Distributed Model Predictive Control algorithm is designed to solve the parameter uncertainty problem in the light-thermal interconnected power system.

(1) Based on the real-time information of the current state of the system, the nominal system is optimized in real time under the control of DMPC so that the system state can change around the determined state trajectory;
(2) Multiple controller gain optimization feedback control laws are employed, enabling the flexible adjustment of weights associated with different Tube models to identify the most effective control law;
(3) The feedback control law integrates the state of adjacent areas, facilitating inter-regional communication and coordinated control. This ensures consistency in system states across areas and enables collaborative responses to external disturbances.

2 Description of the System

2.1 Load Frequency Control Model of Interconnected Power System

The load frequency control model for the interconnected power system in the two areas of the solar-thermal power system is established. Area 1 is composed of the solar-thermal unit and the thermal power unit. The LFC model of the solar-thermal unit is composed of the collector, the governor, the turbine and the generator, and the output power is changed by adjusting the opening of the turbine valve [8, 9]. Area 2 contains a thermal power unit consisting of a governor, a reheat turbine and a generator. Each area is independently regulated by an RDMPC, with information exchanged between areas via the tie-line to maintain stable frequency and power exchange levels. The system structure is shown in Figure 1, and the meanings of each parameter are shown in Table 1.

Area 1 faces uncertainty primarily due to parameter variations resulting from the integration of the Solar thermal generator system, where coefficient matrix parameters fluctuate A_{11}, B_{11}, F_{11} with light intensity ΔI. In contrast, area 2, consisting of conventional units, experiences minimal uncertainties.

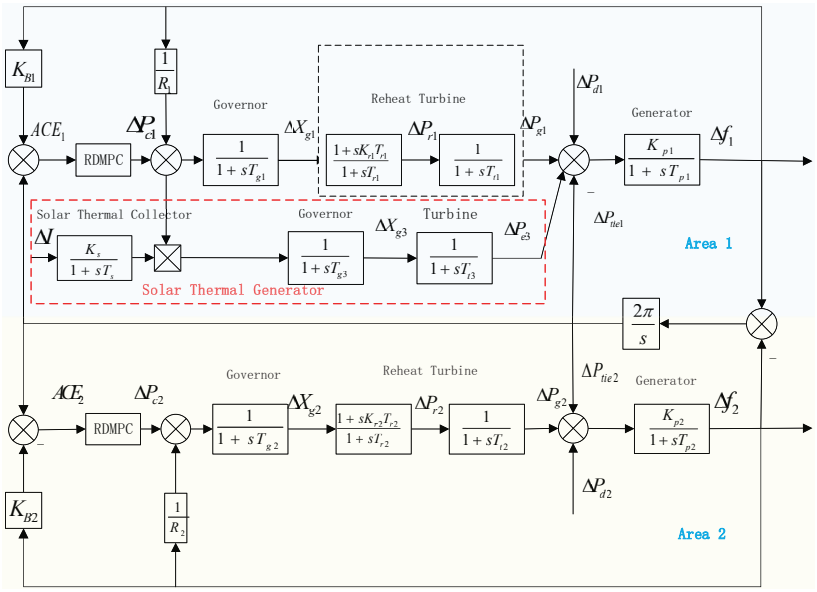

Figure 1 Load frequency control model of ST–Thermal power system.

Table 1 The parameters and variables of power system

Parameters/ Variables	Nomenclatures	Parameters/ Variables	Nomenclatures
Δf	Frequency deviation	K_c	Collector gain
ΔP_g	Generator output power deviation	T_c	Collector time constant
ΔP_{tie}	Tie-line active power deviation	T_t	Turbine time constant
ΔX_g	Governor valve position deviation	T_g	Thermal governor time constant
ΔP_r	Reheat output power deviation	K_s	Control area interaction gain
ΔP_d	Load disturbance deviation	R	Speed droop
ΔP_e	Output power deviation of ST power plant	ACE	Area Control Error
K_p	Power system gain	K_B	Frequency deviation factor
K_r	Reheat gain		

However, real-time communication among areas via liaison lines introduces coupling between adjacent systems. Consequently, changes in one area affect adjacent ones, resulting in fluctuations in the overall power system frequency.

In interconnected power systems, illumination intensity variation is intricate, and uncertainties wield significant influence. To address this, multiplicative uncertainty is transformed into additive uncertainty for processing [8], forming the basis for constructing a robust distributed controller. This controller is coupled with the LFC model (1) of the ST-thermal interconnected power system, enabling the expression of the discrete system's state space as follows:

The LFC model for the i area can be written as:

$$\begin{cases} \dot{x}_i(t) = A_{ii}(t)x_i(t) + B_{ii}(t)u_{ti}(t) + F_{ii}(t)w_i(t) \\ \qquad\qquad + \sum_{i \neq j}(A_{ij}(t)x_j(t) + B_{ij}(t)u_j(t) + F_{ij}(t)w_j(t)) \\ y_i(t) = C_{ii}(t)x_i(t) \end{cases} \tag{1}$$

where, j indicates the adjacent area. The power deviation of interregional contact lines can be written as:

$$\Delta P_{tie}^{ij} = \frac{2\pi}{s} \sum K_{sij}(\Delta f_i - \Delta f_j).$$

Select the state variable of the ST - thermal power area as:

$$x_1 = \begin{bmatrix} \Delta f_1 & \Delta P_{tie1} & \Delta P_{g1} & \Delta X_{g1} & \Delta P_{r1} & \Delta P_{e2} & \Delta X_{g3} & \Delta \dot{X}_{g3} \end{bmatrix}^T$$

The state variables of the thermal power area is:

$$x_2 = \begin{bmatrix} \Delta f_2 & \Delta P_{tie2} & \Delta P_{g2} & \Delta X_{g2} & \Delta P_{r2} \end{bmatrix}^T$$

The input variables, disturbance variables and output variables of all areas are:

$$u_i = \Delta P_{ci}, w_i = \Delta P_{di}, y_i = ACE_i.$$

The coefficient matrix of thermal power area is:

$$A_{22} = \begin{bmatrix} -\frac{1}{T_{p2}} & -\frac{K_{p2}}{T_{p2}} & \frac{K_{p2}}{T_{p2}} & 0 & 0 \\ K_{21} & 0 & 0 & 0 & 0 \\ 0 & 0 & -\frac{1}{T_{t2}} & 0 & \frac{1}{T_{t2}} \\ -\frac{1}{R_2 T_{g2}} & 0 & 0 & -\frac{1}{T_{g2}} & 0 \\ -\frac{K_r}{R_2 T_{g2}} & 0 & 0 & \frac{1}{T_{g2}} - \frac{K_r}{T_{g2}} & -\frac{1}{T_{r2}} \end{bmatrix},$$

$$B_{22} = \begin{bmatrix} 0 & 0 & 0 & \frac{1}{T_{g2}} & 0 \end{bmatrix}^T$$

$$F_{22} = \begin{bmatrix} -\frac{K_{p2}}{T_{p2}} & 0 & 0 & 0 & 0 \end{bmatrix}^T, \quad C_{22} = \begin{bmatrix} K_{B2} & 1 & 0 & 0 & 0 \end{bmatrix}$$

The coefficient matrix of the ST-thermal power area is:

$$B_{11}(t) = \begin{bmatrix} 0 & 0 & 0 & \frac{1}{T_{g1}} & \frac{K_{r1}}{T_{g1}} & 0 & 0 & \frac{K_c \Delta I(t)}{T_c T_{g2}} \end{bmatrix}^T,$$

$$F_{11}(t) = \begin{bmatrix} \frac{K_{p2}}{T_{p2}} & 0 & 0 & 0 & 0 & 0 & 0 & 0 \end{bmatrix}^T,$$

$$C_{11}(t) = \begin{bmatrix} K_{B1} & 1 & 0 & 0 & 0 & 0 & 0 & 0 \end{bmatrix}^T$$

$$A_{11}(t) = \begin{bmatrix} -\frac{1}{T_{p2}} & -\frac{K_{p2}}{T_{p2}} & \frac{K_{p2}}{T_{p2}} & 0 & 0 & \frac{K_{p2}}{T_{p2}} & 0 & 0 \\ K_{12} & 0 & 0 & 0 & 0 & 0 & 0 & 0 \\ 0 & 0 & -\frac{1}{T_{t1}} & 0 & \frac{1}{T_{t1}} & 0 & 0 & 0 \\ -\frac{1}{R_1 T_{g1}} & 0 & 0 & -\frac{1}{T_{g1}} & 0 & 0 & 0 & 0 \\ \frac{K_{r1}}{R_1 T_{r1}} & 0 & 0 & a_2 & -\frac{1}{T_{r1}} & 0 & 0 & 0 \\ 0 & 0 & 0 & 0 & 0 & -\frac{1}{T_{t3}} & \frac{1}{T_{t3}} & 0 \\ 0 & 0 & 0 & 0 & 0 & 0 & 0 & 1 \\ a_1 & 0 & 0 & 0 & 0 & 0 & -\frac{1}{T_c T_{g3}} & a_3 \end{bmatrix}$$

where,

$$a_1 = -\frac{K_c \Delta I(t)}{R_1 T_c T_{g3}}, \quad a_2 = \frac{1}{T_{r1}} - \frac{K_{r1}}{T_{r1}}, \quad a_3 = -\frac{T_c + T_{g3}}{T_c T_{g3}}.$$

The correlation matrix is $A_{ij}(2,1) = -K_{sij}, B_{ij} = 0$.

2.2 System Uncertainty Analysis

Area 1 faces uncertainty primarily due to parameter variations resulting from the integration of the Solar thermal generator system, where coefficient matrix parameters fluctuate A_{11}, B_{11}, F_{11} with light intensity ΔI. In contrast, area 2, consisting of conventional units, experiences minimal uncertainties. However, real-time communication among areas via liaison lines introduces coupling between adjacent systems. Consequently, changes in one area affect adjacent ones, resulting in fluctuations in the overall power system frequency.

In interconnected power systems, illumination intensity variation is intricate, and uncertainties wield significant influence. To address this, multiplicative uncertainty is transformed into additive uncertainty for processing [8], forming the basis for constructing a robust distributed controller. This controller is coupled with the LFC model (1) of the ST-thermal interconnected power system, enabling the expression of the discrete system's state space as

follows:

$$\begin{cases} x_i(k+1) = (\hat{A}_{ii} + \Delta\hat{A}_{ii})x_i(k) + (\hat{B}_{ii} + \Delta B_{ii})(k)u_{ii}(k) + F_{ii}w_i(k) \\ \qquad\qquad + \sum_{i \neq j}(A_{ij}x_j(k) + B_{ij}u_j(k) + F_{ij}w_j(k)) \\ y_i(k) = C_{ii}x_i(k) \end{cases} \tag{2}$$

where $A_{ii} = \hat{A}_{ii} + \Delta A$, $B_{ii} = \hat{B}_{ii} + \Delta B$, $\hat{A}_{ii}$, $\hat{B}_{ii}$ represents the mean value of the uncertain parameters, while ΔA, ΔB denotes the deviation resulting from uncertainty at k specific moments.

3 Tube-based Distributed MPC

"Tube" can be thought of as a zone delimited by upper and lower limits. It centers on the state trajectory of the nominal system and the actual system [10]. The error in the state variable of the nominal system serves as the radius determining the deviation of the actual system's state within this zone, as illustrated in Figure 2. In this method, all uncertainties are separated from the actual system. From this, the remaining deterministic part is defined as the nominal system. The optimal control sequence is obtained by solving the optimization problem of the nominal system. Thus, the control problem of the actual system is transformed into the control of the nominal system; The feedback control law is designed to guide the state of the actual system to the desired location [11, 12].

The Tube-based Distributed Model Predictive Controller consists of two main components: DMPC and the distributed feedback control law. Serving as the core controller group, the distributed model predictive controller focuses on solving the optimization control problem of the nominal system online [13]. By leveraging real-time information about the current system state, DMPC can generate optimal control sequences dynamically. This enables the system to adjust its state trajectory in response to changes, thereby achieving dynamic system adjustments. The distributed feedback control law compensates for deviations between the nominal and actual trajectories. Its components include the system error feedback signal and feedback values from state quantities in adjacent areas. This design facilitates communication and coordinated control between areas, ensuring consistency in system states and coordinated responses to external disturbances. Subsequently, the DMPC

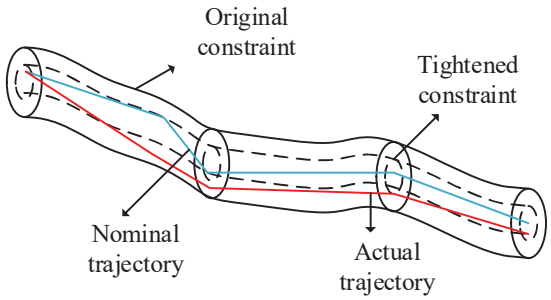

Figure 2 The concept diagram of Tube.

algorithm and the distributed feedback control law for the nominal system are described separately [14].

3.1 Design of DMPC Algorithm for Nominal System

The nominal system encompasses all identified components of the actual system. In the ST-thermal power interconnection system, the sources of uncertainty comprise the system parameter variation term, and the coupling effect of adjacent power generation areas: To simplify, all uncertain components within the system are disregarded, and the average value of the system parameter matrix is selected. The nominal system model can be expressed as follows:

$$z_i(k+1) = \hat{A}_{ii} z_i(k) + \hat{B}_{ii} v_i(k) + F_{ii} w_i(k) \tag{3}$$

where, $z_i(k)$ is the nominal system state variable, $v_i(k)$ is the nominal system control variable, $z_i(k) \in X_i', v_i(k) \in U_i'$, X_i', U_i' is a tightened set of constraints, $w_i(k)$ is the nominal system disturbance variable. In interconnected power systems: $w_i(k) = \Delta P_{di}(k)$.

The DMPC algorithm is employed to solving the Load Frequency Control issue within the nominal system. The optimization goal of the local controller within the system is to regulate the output of the generator set in the local area to accommodate load fluctuations and uphold the system frequency at the designated value. The objective function of the nominal system for each area can be defined as follows:

$$\min J_i(k) = \sum_{p=1}^{N_p} \|z_i(k+p|k)\|_{Q_i}^2 + \sum_{q=1}^{N_c} \|v_i(k+q|k)\|_{R_i}^2 \tag{4}$$

where, Q_i, R_i, S_i is weight matrix. By resolving the DMPC optimization problem of the nominal system, the optimal control magnitude of the nominal system can be acquired devoid of any uncertainty, thereby ensuring the system state steadily attains the desired value.

The error system delineates the deviation in state quantity between the actual system and the nominal system:

$$e_i(k) = x_i(k) - z_i(k) \tag{5}$$

3.2 Distributed Feedback Control Law

The distributed feedback control law compensates for the error between the real trajectory and the nominal trajectory by using the system state deviation and adjacent area information, so as to realize the real-time monitoring and adjustment of the system state. Simultaneously, integrating the states of adjacent areas into the feedback control law facilitates effective coordination between areas.

The algorithm framework of standard Tube DMPC is depicted in Figure 3. It employs a blend of nominal system and fixed feedback control law, integrating state information from adjacent areas into the feedback term. Under the standard Tube DMPC policy, the input to the actual system is:

$$u_i(k) = v_i(k) + K_{ii}e_i(k) + \sum_{j \neq i} K_{ij}x_j(k) \tag{6}$$

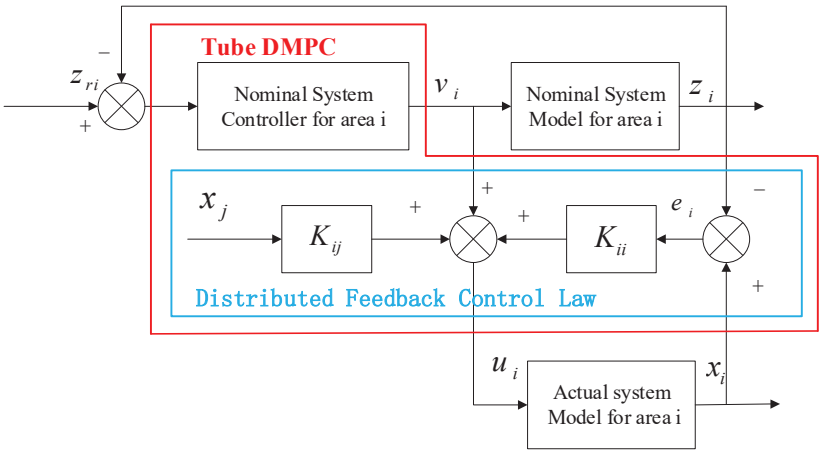

Figure 3 Standard Tube DMPC algorithm framework.

According to formula (4), (5) and (8), it can be obtained that under the control of standard Tube DMPC, the error system at the time is as follows:

$$\begin{aligned} e_i(k+1) &= x_i(k+1) - z_i(k+1) \\ &= (\hat{A}_{ii} + \hat{B}_{ii}K_{ii})e_i(k) + \Delta A x_i(k) + \Delta B u_i(k) \\ &\quad + \sum_{j \neq i} (A_{ij} + \hat{B}_{ii}K_{ij})x_j(k) \end{aligned}$$

Thus, the dynamics of the error system can be described as:

$$e_i(k+1) = \Phi_{ii} e_i(k) + \omega_i(k) \tag{7}$$

where, $e_i(k) \in E_i$, $\Phi_{ii} = \hat{A}_{ii} + \hat{B}_{ii}K_{ii}$, $\Phi_{ij} = A_{ij} + \hat{B}_{ii}K_{ij}$, $\omega_i(k) = \Delta A x_i(k) + \Delta B u_i(k) + \sum_{j \neq i} \Phi_{ij} x_j(k)$, $\omega_i(k)$ is the disturbance of the error system, contains all the uncertain parts of the system. For ST-thermal interconnected power systems:

area 1: $\omega_i(k) = \Delta A x_i(k) + \Delta B u_i(k) + \sum_{j \neq i} \Phi_{ij} x_j(k)$
area 2: $\omega_i(k) = \sum_{j \neq i} \Phi_{ij} x_j(k)$

The feedback gain value K_{ii} affects the stability of the system, which can be obtained by solving the following formula:

$$\begin{aligned} K_{ii} &= (R_i + B_{ii}^T \hat{P}_i B_{ii})^{-1} B_{ii}^T \hat{P}_i A_{ii} \\ \widehat{P}_i &= A_{ii}^T \hat{P}_i A_{ii} + Q_i - A_{ii}^T \hat{P}_i B_{ii} (R_i + B_{ii}^T \hat{P}_i B_{ii})^{-1} B_{ii}^T \hat{P}_i A_{ii} \end{aligned} \tag{8}$$

Under the combined influence of DMPC and the feedback control law, the system's dynamic error can be constrained within a Robust Positively Invariant Set: E_i, thereby confining the actual system's state within a Robust Positively Invariant Set with the nominal system's state trajectory as its center and size. To alleviate the conservatism of standard Tube DMPC, according to Equation (7), the disturbance variable of the error subsystem needs to be updated at each instance based on the state and input variables from the previous instance. Consequently, the disturbance set is updated. Set the initial time error system $W_i(k) = \Delta A X_i + \Delta B U_i$.

To streamline the solution process for the Robust Positively Invariant Set amidst parametric uncertainties in interconnected power systems, a multiplication-variable-addition transformation is implemented. While this transformation simplifies the construction of the robust invariant set, it also

enlarges the uncertainty set. Due to the fixed-gain feedback control law employed in standard Tube DMPC, the expanded uncertainty set diminishes the controller's performance, and in some cases, renders finding a feasible solution unattainable, thereby hindering the achievement of control objectives. Additionally, the operational requirements of power systems are intricate, particularly when there are frequent fluctuations in light intensity, necessitating coordinated output adjustments between solar thermal units and thermal power plants to regulate frequency. Conversely, during minimal fluctuations in light intensity, greater power output from photothermal units is required to accommodate load changes, thereby reducing the output of thermal power units and lowering carbon emissions. To address these challenges, a Hybrid Multi-Tube DMPC algorithm is proposed to enhance control performance and bolster system stability.

Hybrid Multi-Tube DMPC is a strategy that combines multiple standard Tube DMPC to more comprehensively adapt to the dynamic characteristics of the controlled object. Its algorithm framework is shown in Figure 4. In this control strategy, the error system is decomposed into multiple error subsystems. By designing distributed feedback control laws with different gain values, robust positive invariant sets satisfying different control requirements are constructed, and the weights of different tubes are flexibly adjusted according to the operating characteristics of the system, so as to achieve more accurate control of the controlled object.

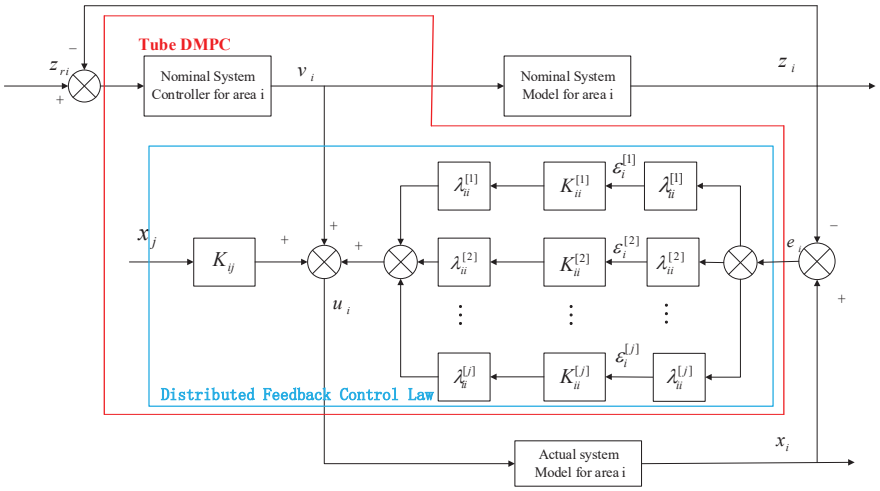

Figure 4 Hybrid Multi-Tube DMPC algorithm framework.

The error system is $e_i(k)$ decomposed into multiple error subsystems with weight coefficients of $\lambda_{ii}^{[j]}$:

$$e_i(k) = \sum_{j=1}^{M} \lambda_i^{[j]} \varepsilon_i^{[j]}(k) \tag{9}$$

where $1 \leq j \leq M$, $\sum_{j=1}^{M} \lambda_i^{[j]} = 1$ Select M different feedback controller gains $K_{ii}^{[1]}, K_{ii}^{[2]}, \ldots K_{ii}^{[M]}$, each $K_{ii}^{[j]}$ corresponding to an error subsystem $\varepsilon_{ii}^{[j]}(k)$, the dynamic model of the error subsystem can be written as:

$$\varepsilon_i^{[j]}(k+1) = (\hat{A}_{ii} + \hat{B}_{ii} K_{ii}^{[j]}) \varepsilon_i^{[j]}(k) + \omega_i(k) \tag{10}$$

The feedback control law comprises a standard online combination of tubes with various gain values. To optimize the control effectiveness, the weights of different Tube models can be adjusted flexibly to identify the most suitable control law. The input to the actual system is:

$$u_i(k) = v_i(k) + \sum_{j=1}^{M} \lambda_i^{[j]} K_{ii}^{[j]} \varepsilon_i^{[j]}(k) + \sum_{j \neq i} K_{ij} x_j(k) \tag{11}$$

Hybrid Multi-Tube DMPC customizes various feedback controller gains to suit diverse control needs, dynamically tunes the weights of different Tube models based on the system's operational state, fully exploits the benefits of Hybrid Multi-Tube approaches, enhances the system's flexibility to adapt to real-world changes, and fortifies the robustness of the control algorithm in the power system.

As per the stability theorem, it's essential to ensure the stability of the error subsystem under various feedback control laws, necessitating that $K_{ii}^{[j]}, K_{ij}$ meets the requirements [15]:

$$\sum_{j \neq i} \sum_{r=0}^{\infty} \| (\hat{A}_{ii} + \hat{B}_{ii} K_{ii}^{[j]})_{ii}^{r} \Phi_{ij} \|_{\infty} < 1 \tag{12}$$

Solving the Robust Positive Invariant Set

The specific process for solving robust invariant sets is as follows:

First, the perturbation set of the error system is transformed into the following: $W_i \triangleq \{\omega_i \in \Re^n | f_i^T \omega = g_i\}$. According to the definition of the robust

positive invariant set approximation, α depends on s. For any s, $\alpha(s) = max\ sup\frac{(\Phi_{ii}^{s})^{T} f_i}{g_i}$. Then, let $\alpha = 0$ be such that it attains the minimum value of s satisfying the approximation of the robust positive invariant set. When the values of the two satisfy $\oplus_{j=0}^{s-1}\Phi_{ii}^{j} W_i \subseteq \alpha^{s}(1-\alpha)B_p(\eta)$, α, s represents the solution of the robust positive invariant set. The final robust invariant set is obtained by substituting them into Equation (11), where $B_p(\eta) = \{\|x_i\|_p = \eta\}$ and η are preset parameters reflecting the approximation accuracy of the invariant set.

According to Equations (11) and (12), it can be obtained that under mixed multi-tube DMPC control, the robust positive invariant set of system error is [16]:

$$E_i = (1-\alpha)^{-1} \bigoplus_{j=0}^{s-1} \Phi_{ii}^{j} W$$

$$E_i^{[j]} = (1-\alpha)^{-1} \bigoplus_{m=0}^{s-1} (\hat{A}_{ii} + \hat{B}_{ii} K_{ii}^{[j]})^{m} W \tag{13}$$

where E_i' is the robust positive invariant set of the regional system, $\oplus$ represents the set Minkowski and where Θ represents the Pontriagin set difference.

3.3 Algorithm Flow

The control goal of the nominal system becomes to solve the appropriate v, λ so that the cost function is minimized:

$$z_i(k+1) = \hat{A}_{ii} z_i(k) + \hat{B}_{ii} v_i(k) + D\Delta P_{di}$$

$$z_i(k) = x_i(k)$$

$$z_i(k+p|k) \in X_i' = X_i \Theta E_i'$$

$$v_i(k+q|k) \in U_i' = U_i \Theta \left(\bigoplus^{j=1_M} K_{ii}^{[j]} \lambda_{ii}^{j} E_i^{[j]} \oplus K_{ij} X_j \right) \tag{14}$$

The algorithm flow of Hybrid Multi-Tube distributed model predictive control is as follows:

Offline section:

The weight coefficient matrix Q_i, R_i is given, M gains K_{ii} are obtained for each area, and K_{ij} satisfying the condition is calculated.

Online section:

(1) Set the initial parameters of the initial moment: $z_i(0) = x_i(0)$
(2) Each subsystem exchanges information about each other x_i, z_i
(3) According to the disturbance w_i of each subsystem at this time, the corresponding robust invariant set E_i' is obtained, and the optimization problem (14) is solved to obtain the control quantity $v_i(k)$ and the appropriate λ of the nominal system
(4) According to the feedback control law, the control quantity of the actual system $u_i(k)$ is obtained and input into the system. At the next moment $k + 1$, repeat the above steps.

4 Simulated Analysis

In the proposed light-heat-thermal interconnected power system, illustrated in Figure 1, Tube DMPC is employed for simulation research. The proposed control algorithm is compared with DMPC and standard Tube DMPC to validate its effectiveness.

Referring to the actual fluctuation of light intensity, the following simulation scenarios are set:

Case 1: With constant light intensity and load disturbances occurring in the system, the load frequency of the interconnected power system is controlled. This case verifies that robust distributed predictive control can maintain effective control even when parameters remain unchanged.

Case 2: The load frequency control process of the interconnected power system when light intensity fluctuates randomly within a certain range and load disturbances occur in the system.

The sampling time is set to $T_s = 0.01s$, and the prediction and control time domains are set to $N_p = 5, N_c = 3$. The values of other parameters are detailed in Table 2, with weighted matrices Q_i and R_i:$Q_1 = diag(1000 \quad 10 \quad 0.001 \quad 0.001 \quad 0.001)$, $R_1 = R_2 = 0.01$

$$Q_2 = diag(1000, 10, 0.001, 0.001, 0.001, 0.001, 0.001, 0.001).$$

The gain value of the standard Tube DMPC feedback control law can be obtained by Equation (10), and the nominal system solves the following

Table 2 Parameters and values of the power system

$K_{pi} = 120Hz/p.u.MW, T_{pi} = 20s, T_{gi} = 0.08s, T_{ti} = 0.3s$
$K_{ri} = 0.5Hz/p.u.MW, T_{ri} = 10s, R_i = 2.4Hz/p.u.MW$
$K_c = 1.8Hz/p.u.MW, T_{ci} = 1.8s, K_{sij} = 0.545p.u.MW$

optimization problems:

$$min\ J_i(k) = \sum_{p=1}^{N_p} \|z_i(k+p|k)\|_{Q_i}^2 + \sum_{q=1}^{N_c} \|v_i(k+q|k)\|_{R_i}^2$$

$$z_i(k+1) = \hat{A}_{ii} z_i(k) + \hat{B}_{ii} v_i(k) + F_{ii} \Delta P_{di}(k), z_i(k) = x_i(k)$$

$$z_i(k+p|k) \in X_i' = X_i \Theta E_i$$

$$v_i(k+q|k) \in U_i' = U_i \Theta (\oplus K_{ii} E_i \oplus K_{ij} X_j)$$

$$E_i = (1-\alpha)^{-1} \bigoplus_{m=0}^{s-1} (\hat{A}_{ii} + \hat{B}_{ii} K_{ii})^m W \tag{15}$$

The Hybrid Multi-Tube DMPC provides three distinct sets of controller gain values, denoted as $K_{ii}^{[j]}, K_{ij}$. The value $K_{ii}^{[1]}$, derived from formula (11), is applicable to standard scenarios where each system adjusts unit output in the area to accommodate load changes. The value $K_{ii}^{[2]}$ is suitable for scenarios with frequent changes in light intensity, where the system needs to promptly adjust the output of the solar thermal unit to mitigate frequency fluctuations and coordinate thermal power output to maintain grid frequency stability. On the other hand, the value $K_{ii}^{[3]}$ is appropriate for releasing more power from the photothermal unit in response to minor fluctuations in light intensity. Refer to Table 3 for the gain matrix values in each area. In various scenarios, the nominal system solves the control problem (14), adjusting different Tube weights online to dynamically adapt to the power system's characteristics.

By utilizing the MPPT toolbox in MATLAB to solve formula (14), the corresponding robust positive invariant set can be obtained, which is then integrated into the feedback controller (11) to facilitate system control.

4.1 Constant Light Intensity

With constant light intensity, a load disturbance of $0.01p.u.$ is applied to area 1 at $t = 30s$, and a load disturbance of $-0.015p.u.$ is applied at

Table 3 Values of the power system gain matrix

$K_{11}^{[1]} = [-0.1585, 0.5238, -0.1705, 0.4141, -0.3607, -0.3324, -0.5345, -0.0427]$
$K_{12}^{[2]} = [-0.1900, 0.5757, -0.2514, 0.4209, -0.3250, -1.8280, -1.4698, -0.8938]$
$K_{13}^{[3]} = [-11.3595, -1.8527, 2.0845, 0.1421, -0.2158, 2.0349, -2.6191, -12.8840]$
$K_{12} = [-0.0099, 0.0099, -0.0099, 0.0094, -0.01, -0.01, 0.0094, 0.0099]$
$K_{22}^{[1]} = [-655.79 \quad 301.16 \quad -283.47 \quad 5.16 \quad -40.11]$
$K_{22}^{[2]} = [-25.14 \quad 24.06 \quad -10.02 \quad 6.04 \quad -1.00]$
$K_{22}^{[3]} = [-1.00 \quad 6.04 \quad -10.02 \quad 24.06 \quad -25.14]$
$K_{21} = [-0.0099 \quad 0.0099 \quad -0.0099 \quad 0.0094 \quad -0.01]$

$t = 80s$. DMPC and Hybrid Multi-Tube DMPC are employed to control the load frequency of the interconnected power system. The effectiveness of load frequency control in the power system is verified while ensuring that the design of the Hybrid Multi-Tube does not influence parameter determination. The frequency response process of each area is outlined below.

With constant light intensity, the power output of the photothermal unit remains stable, resulting in zero frequency deviation across each area of the power system. However, at 30 seconds, an increase in the load of area 1 causes a system power imbalance, leading to significant frequency fluctuations in area 1. This imbalance also triggers frequency deviations in area 2 due to inter-area connections via liaison lines. Concurrently, units in each area coordinate their actions to collectively respond to the load change.

As depicted in Figures 5 and 6, under the Hybrid Multi-Tube DMPC strategy, the system's frequency deviation stabilizes at $\pm$0.006Hz. This demonstrates an equivalent control effectiveness to DMPC, ensuring the stability of the power system. In essence, Hybrid Multi-Tube DMPC maintains optimal control effectiveness even when parameters remain unchanged.

4.2 Light Intensity Varies Randomly

The random variation curves of light intensity are illustrated in Figure 7. At $t = 30s$, a load disturbance of $0.01p.u.$ is applied to area 1, followed by a load disturbance of $-0.015p.u.$ at $t = 80s$. These disturbances were introduced to area 1 to assess the superior control efficacy of Hybrid Multi-Tube DMPC when power system parameters undergo changes.

Figures 8 and 9 depict the comparison of frequency response curves across different areas of the mixed multi-tube DMPC and standard Tube

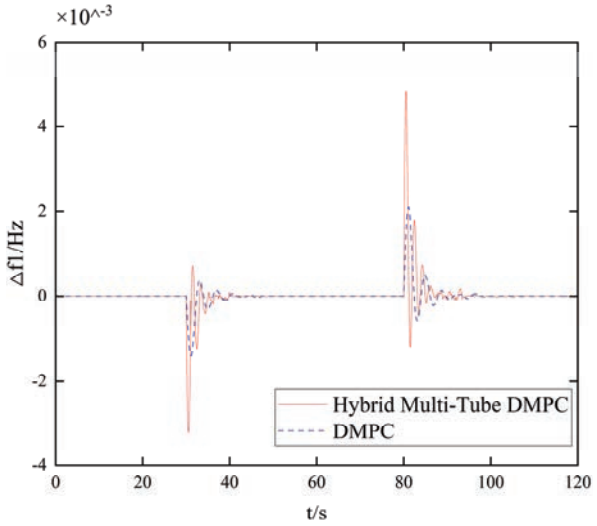

Figure 5 Frequency response curve of area 1 with no change in light intensity.

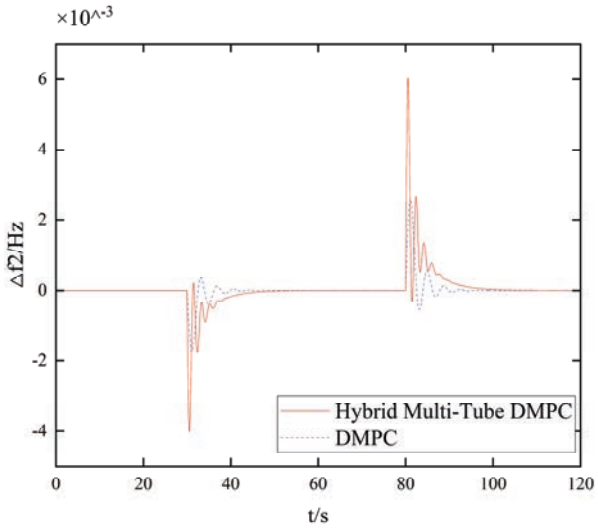

Figure 6 Frequency response curve of area 2 with no change in light intensity.

DMPC under parameter variations. Throughout the interval from 0 to 30 seconds, the loads in each area remain constant. However, due to the non-empty disturbance invariant set of the error system, which is continuously updated based on the system state, the system frequency deviation undergoes

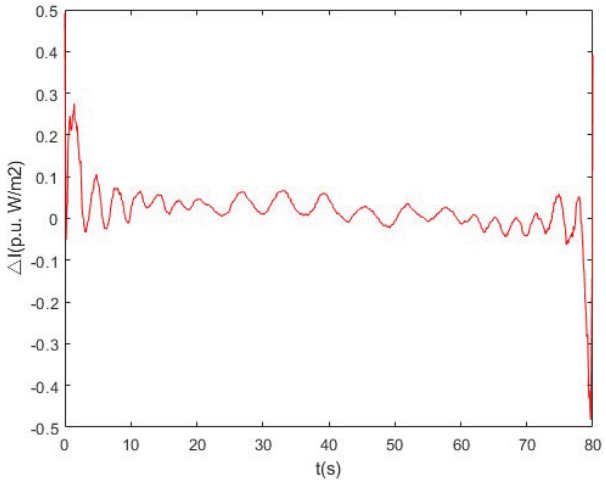

Figure 7 Random variation curve of light intensity.

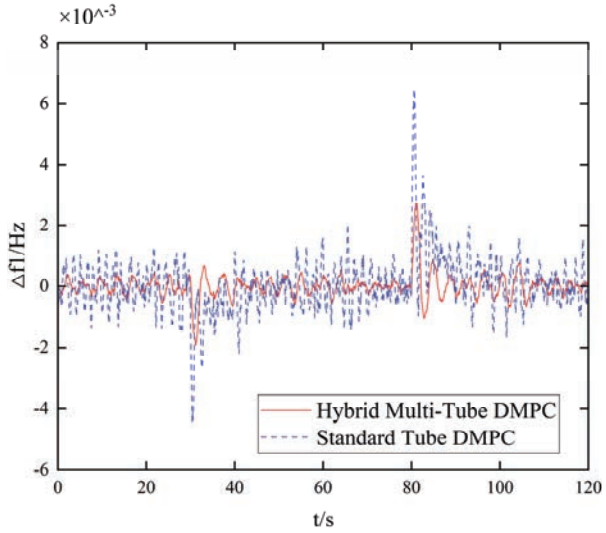

Figure 8 Frequency response curve of area 1 under random changes in light intensity.

continuous changes. The regional controllers collaborate to regulate the output power in each area and collectively participate in frequency modulation to meet the load demand.

At $t = 30s$, the load in area 1 experiences a $0.01p.u.$ increment, leading to a significant fluctuation in the power grid frequency. Through inter-regional

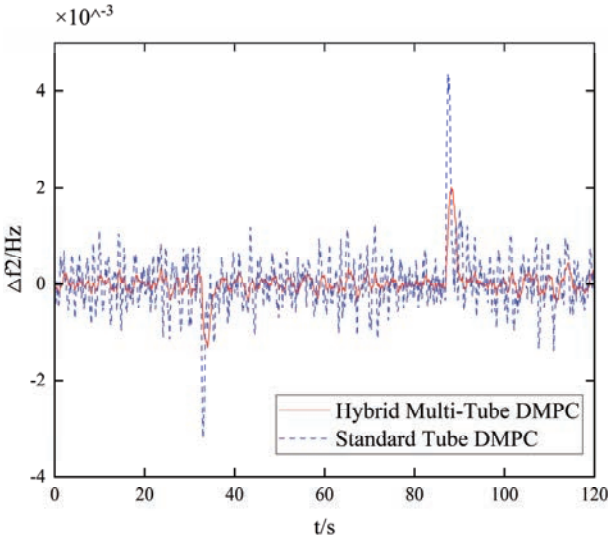

Figure 9 Frequency response curve of area 2 under random changes in light intensity.

communication facilitated by the liaison line, the output of the thermal power area also increases proportionally. Collaboratively suppressing the impact of disturbances with the output of the light-thermal power area, the frequency deviation of each area is controlled within ± 0.005. Notably, as depicted in Figures 8 and 9, the system frequency exhibits frequent fluctuations under the control of standard Tube DMPC, with significant fluctuations observed during the latter stages of the frequency modulation process.

In contrast, the frequency response curve of the Hybrid Multi-Tube DMPC control strategy proposed in this paper exhibits less fluctuation, faster adjustment speed, and better tracking effect, thereby enhancing the robustness of the control algorithm in the interconnected power system.

5 Conclusion

This paper proposes a load frequency control strategy based on Tube DMPC to address the uncertainties in system parameters arising from changes in light intensity. Initially, the LFC model for the interconnected power system spanning two areas, namely photothermal and thermal power, is established. The photothermal system governs output power by adjusting the turbine valve opening and actively participates in system frequency modulation. The

variations in model parameters resulting from fluctuations in illumination intensity are treated as uncertainty disturbances.

To mitigate solving complexity, parameter uncertainties are transformed into additive uncertainties by estimating the mean value and maximum deviation of the parameters. The controller adopts a combination of DMPC and feedback control law: DMPC handles the control of the undisturbed system and determines the optimal solution in response to load variations in the power system. The feedback control law employs a standard Tube online combination with varying gain values, allowing for flexible adjustment of the weights of different Tube models to identify the optimal control law. Furthermore, the design includes a state feedback component for adjacent areas to facilitate inter-regional communication, enabling the actual system state to continually track the set value.

Simulation results demonstrate that the Hybrid Multi-Tube DMPC effectively mitigates frequency fluctuations in the power system, resulting in smoother frequency response curves and demonstrating strong control efficacy.

References

[1] Mohsen Babaei, Mohsen Hadian. Learning-based Fractional Order PID Controller for Load Frequency Control of Distributed Energy Resources Including PV and Wind Turbine Generator[J]. Distributed Generation & Alternative Energy Journal, 2022,37(6):1755–1772.

[2] Yatin Sharma, Lalit Chandra Saikia, Automatic generation control of a multi-area ST – Thermal power system using Grey Wolf Optimizer algorithm based classical controllers [J]. International Journal of Electrical Power & Energy Systems, 2015(73): 853–862.

[3] Nong Huiyun. Distributed Model Predictive Control with Application to Load Frequency Control System[D], 2015(in Chinese).

[4] Zhang Yi, Chang Pengfei. Load Frequency Control of Multi-area Interconnected Power System with Renewable Energy[J]. Industrial Control Computer, 2020, 33(10):47–49 (in Chinese).

[5] Liao Xiaobing; Liu Kaipei; Qin Liang, et al., Cooperative DMPC-Based Load Frequency Control of AC/DC Interconnected Power System with Solar Thermal Power Plant [C]. 2018 IEEE PES Asia-Pacific Power and Energy Engineering Conference (APPEEC), Kota Kinabalu, Malaysia, 2018:341–346.

[6] Zhang Yi, Liu Xiangjie. Robust distributed model predictive control for load frequency control of uncertain power systems[J]. Control Theory & Applications, 2016, 33(5):621–630 (in Chinese).
[7] Liu Xiangjie, Wang Ce, Kong Xiaobin, Zhang Yi, Wang, Weisheng and Lee K. Y., Tube-based Distributed MPC for Load Frequency Control of Power System with High Wind Power Penetration[J], IEEE Transactions on Power Systems, 2023:1–12.
[8] T. Krishnaiah, Dr. S. Srinivasa Rao, Dr. K. Madhu Murthy, Solar Stirling Dish Power Generation Atlas of India[J]. Distributed Generation & Alternative Energy Journal, 2009, 24(2):35–50.
[9] Dr. Sriram Somasundaram, Dr. Kevin Drost, Mr. Daryl R. Brown, Diurnal Thermal Energy Storage for Cogeneration Applications[J]. Distributed Generation & Alternative Energy Journal, 1997, 12(2):35–50.
[10] Mayne D.Q., Kerrigan E.C., Falugi P. Robust model predictive control: advantages and disadvantages of tube-based methods[J]. IFAC Proceedings Volumes, 2011, 44(1): 191–196.
[11] Riverso S., Ferrari-Trecate G. Plug-and-Play distributed model predictive control with coupling attenuation[J]. Optimal Control Applications & Methods, 2015, 3(36): 292–305.
[12] Oshnoei A., Kheradmandi M., Muyeen S.M. Robust control scheme for distributed battery energy storage systems in load frequency control[J]. IEEE Transactions on Power Systems, 2020, 35(6): 4781–4791.
[13] Riverso S, Farina M, Ferrari-Trecate G. Plug-and-play decentralized model predictive control for linear systems[J]. IEEE Transactions on Automatic Control, 2013, 10(58):2608–2614.
[14] Langson W., Chryssochoos I., Rakoviæ S.V., et al. Robust model predictive control using tubes[J]. Automatica, 2004, 40(1): 125–133.
[15] Rakovic S V, Kerrigan E C, Kouramas K I, and Mayne D Q. Invariant Approximations of the Minimal Robust Positively Invariant Set[J]. IEEE Transactions on Automatic Control, 2005, 3(50):406–410.
[16] Dashkovskiy S, Ruffer B S, Wirth F R, An ISS small gain theorem for general networks[J], Mathematics of Control, Signals, and Systems, 2007, 19(2):93–122.

Biography

Wang Xinshan received bachelor's degree in automation from North China Electric Power University in 2021 and master's degree in control science and engineering from North China Electric Power University in 2024. Her research interests include model predictive control and power system load frequency control.